Impact of Radiation Attenuation and Temperature Evolution on Monomer Conversion of Dimethacrylate-based Resins with a Photobleaching Photoinitiator

Veronica Mucci,[1] Wayne D. Cook,[2] Claudia Vallo[1]
[1] *Instituto de Investigación en Ciencia y Tecnología de Materiales, Polymer Department, Mar del Plata University - National Research Council (CONICET), Argentina*

[2] *Department of Materials Engineering, Monash University, Melbourne, Victoria, Australia*

The photopolymerization process of a dimethacrylate copolymer system activated by the camphorquinone (CQ)/amine photoinitiator system (1 wt%), was experimentally studied under nonisothermal conditions in 1- and 2-mm thick samples by measuring double bond conversion, temperature rise and radiation attenuation through the sample during polymerization. The peak temperature in 1- or 2-mm thick samples irradiated at 5 mW/cm^2 was 29 and 38°C, respectively. The temperature evolution during polymerization was also predicted by solving the energy balance coupled with the kinetic expressions for the reaction rate. Radiation attenuation as a function of depth by the photobleachable CQ results in spatial and temporal variation in the local rates of the kinetic steps involved. General relationships for spatiotemporal variations in concentration of a photobleaching initiator, in systems where attenuation and initiator consumption are taken into account, were used to compute local polymerization rates. The effects of radiation attenuation, photobleaching of the photoinitiator and variation of cure temperature at different depths into the resin, all compete to determine the double bond consumption. The increased radiation attenuation in the 2-mm thick sample was accompanied by a higher cure temperature compared with the 1-mm thick sample, and as a result, the monomer conversion averaged over the sample thickness in the 1- and 2-mm thick samples was the same. Results obtained in this research highlight the inherent interlinking of thermal and radiation attenuation effects in bulk photopolymerizing systems. POLYM. ENG. SCI., 49:2225–2233, 2009. © 2009 Society of Plastics Engineers

INTRODUCTION

Light-activated dental composites are commonly used in clinical restorative dentistry. Dimethacrylate copolymers based on 2,2-bis[4-(2-hydroxy-3-methacryloxyprop-1-oxy)phenyl]propane or bisphenol-A diglycidyl ether dimethacrylate (bis-GMA) in combination with a reactive diluents such as triethylene glycol dimethacrylate (TEGDMA) are used as the organic phase of dental restorative composites. Photopolymerization is generally initiated by a camphorquinone (CQ)/amine photoinitiating system, which produces free radicals on exposure to 450–500 nm radiation [1–4].

In many photoinitiated polymerizations, the initiation rate is spatially inhomogeneous and there exists a gradient in polymerization rates [5–7] because the photoinitiator absorbs the radiation and so attenuates, the light intensity as a function of depth along the optical path. Additionally, in most photopolymerization systems, the photoinitiator is photobleached and the light penetrates more deeply into the sample as the photoirradiation continues. The spatially inhomogeneous initiation rates result in a gradient in double bond conversion along the beam direction. Photopolymerization kinetics of dimethacrylate copolymers under isothermal conditions has been widely studied [8–11]; however, the study of the photopolymerization reactions under nonisothermal conditions has not received the same attention despite its significance in real-life applications. The polymerization reaction is highly exothermic, which results in an increase in the sample temperature during the process and this effect becomes more important as the sample thickness increases. The temperature at which the polymerization occurs can have a marked impact on the kinetics of the reaction and the final level of monomer consumption. For this reason, it is relevant to study the combined effect of cure temperature, radiation attenuation and photobleaching in bulk photopolymerizations.

The purpose of this study was to use both experimental and modeling techniques to investigate the photopolymerization of a bis-GMA/TEGDMA resin with CQ photoinitiator in samples of different thickness under

Correspondence to: Claudia Vallo; e-mail: civallo@fi.mdp.edu.ar
Contract grant sponsors: CONICET, ANPCyT.
DOI 10.1002/pen.21460
Published online in Wiley InterScience (www.interscience.wiley.com).

nonisothermal conditions to establish the factors that determine the final double bonds consumption. The local polymerization rate was calculated in terms of the local light intensity and local photoinitiator concentration and these were then used to calculate the temperature evolution during polymerization by solving the energy balance. The cure temperature and light attenuation increase with layer thickness, therefore, both factors compete to determine the final conversion.

MATERIALS AND METHODS

Materials

The resins were formulated from blends of bis-GMA (Esstech, Essington, PA) and TEGDMA (Aldrich) at a mass ratio of 70:30 bis-GMA/TEGDMA. The resins were activated for visible light polymerization by the addition of 1 wt% CQ and an equimolar amount of dimethylaminoethylmethacrylate (DMAEMA, Aldrich). All materials were used as received.

Light Source

The light source used was assembled from a light emitting diode (LED, OTLH-0090-BU, Optotech, Inc.). The relative emission spectrum of the LED source was measured with a calibrated CVI-monochromator (Digikrom 480) and was found to lie within the range 430–520 nm with its spectral emittance centered at 470 nm. The diameter of the irradiation area was 10 mm, which is equal to the diameter of the photocuring sample. The LED was selected to obtain an optimum overlap between the spectral irradiance of the curing unit and the absorption spectrum of CQ (extinction coefficient equal to 42 l mol^{-1} cm^{-1} at the 470 nm absorbance maximum). The absolute, total intensity of the LED was measured with the chemical actinometer, potassium ferrioxalate, which is recommended for the 253–577 nm wavelength range. The irradiance at the base of the photocuring samples was 5 mW/cm^2.

Measurement of Double Bond Conversion

In a previous study [12], a fiber optic sensing method based on a Fizeau-type interferometric scheme had been used to continuously monitor the shrinkage of the photocuring resin during its photoirradiation. Based on the assumption that the shrinkage is proportional to conversion of double bonds, this shrinkage data yielded the evolution of the global (i.e., volume averaged) double bond conversion during the photopolymerization experiment. These conversion data [12] were supplemented here with near-infrared spectroscopy (NIR) measurements of the conversion of partly photocured resin using 1- or 2-mm thick and 10-mm diameter samples of resins prepared with bis-GMA/TEGDMA and CQ/DMAEMA photoinitiator. The resin was sandwiched between two 2-mm thick glass plates separated by a 1- or 2-mm thickness rubber spacer. The assembly was tightly attached to the FTIR sample holder using small clamps. To obtain the double bond conversion as a function of the irradiation time, different samples were irradiated for 10, 20, 30, 40, 60, 80, and 100 s and the NIR spectrum was immediately acquired with a Genesis II Mattson FTIR (Madison, WI) over the range 4500–7000 cm^{-1} from 16 coadded scans at 2 cm^{-1} resolution. The coadded spectra took 120 s to acquire and so any dark reaction occurring during these measurements was negligible. The spectra were corrected by subtraction of a background spectrum collected through an empty mold assembly fitted with only one glass slide to avoid internal reflectance patterns. The conversion profiles were calculated from the decay of the absorption band located at 6165 cm^{-1} [13]. The purpose of this measurement was to validate trends of conversion versus irradiation time in samples of different thickness observed previously by the interferometric technique [12]. Two replicates were used in the measurement of conversion.

Photobleaching of CQ

The DMAEMA amine and bis-GMA/TEGDMA resins do not absorb significantly between 420 and 520 nm so that the photobleaching of the CQ can be assessed by monitoring the decrease in light absorption as a function of continuous irradiation time. The sample of bis-GMA/TEGDMA containing CQ/DMAEMA was contained in a 10-mm diameter well constructed from a rubber gasket material and with a 2-mm thick glass slide (Scheme 1). The thickness of the samples was either 1 ± 0.1

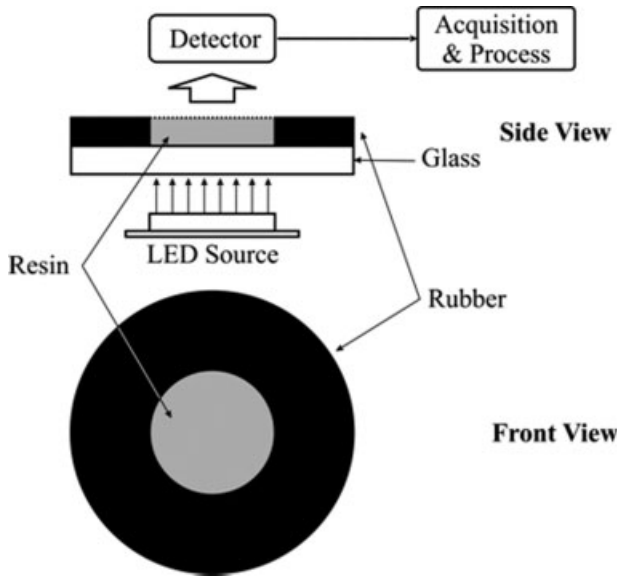

SCHEME 1. Experimental setup for temperature and light transmitted measurements.

 DOI 10.1002/pen

or 2 ± 0.1 mm. The photodetector of the transmitted light was an OPHIR device (OPHIR Optronics, Israel), PD 2000, range 2 μW to 200 mW, precision ±3%. The light source was placed underneath the sample and in contact with the glass slide. The photodetector (10-mm diameter) was placed above and at the centre of the sample at a distance <1 mm to collect and measure the transmitted light as a function of irradiation time. Measurements were also carried out in resins without photoinitiator to correct for the radiation scattered/reflected at the air/glass/resin/air interfaces. It is important to note that the experimental setup is the same as that used in measurements of conversion by the interferometric technique [12]. Three replicates of each test were performed.

Measurement of Temperature Evolution During Photopolymerization

The temperature during polymerization was monitored with fine K-type thermocouples (Omega Engineering, Inc., USA) embedded in the resin specimens in the upper half of the sample where the temperature is more uniform. This was verified after the experiment by visual examination of the sample with a magnifying lens. The thermocouples were connected to a data acquisition system that registered temperature every second. The samples were irradiated for 320 s and the data acquisition continued with the LED unit turned off to complete the 600 s experimental period. Four replicates were conducted for each experiment. The sample thickness was either 1 or 2 mm. The irradiance at the base of the sample was 5 mW/cm^2.

Energy Balance

The heat generated by the exothermic polymerization reaction results in an increase of the temperature in the resin. The local temperature for a given time is related to the heat production rate and the heat transfer rate as stated by the general energy balance, which in cylindrical coordinate system is given by [14]:

$$\rho C_p \frac{\partial T}{\partial t} = \lambda \left(\frac{\partial^2 T}{\partial z^2} + \frac{1}{r}\frac{\partial T}{\partial r} + \frac{\partial^2 T}{\partial r^2} \right) + \Delta H \rho \frac{\partial x}{\partial t} + \varepsilon I \mathrm{CQ} \quad \left(\frac{\mathrm{J}}{\mathrm{m}^3/\mathrm{s}} \right) \tag{1}$$

where T is the temperature, z is the distance from the irradiated surface, r is the radial distance from the central axis of the mold, and t is the time. The resin and mold properties involved are the extent of reaction (x), the thermal conductivity (λ), the mass density (ρ), and the specific heat per unit mass (C_p) (Table 1). ΔH is 275 J/g based on the composition of the resin and the heat of methacrylate polymerization (57.8 kJ/mol [9]). I is the local light irradiance, CQ is the local concentration of the absorbing CQ photoinitiator, and ε is the absorption coefficient of CQ. The heat production and heat transference rates during polymerization were assumed to be nonuniform, that is, depending on the local temperature and local monomer conversion. The following boundary conditions and time condition were used:

TABLE 1. Physical and thermal properties of the materials involved in Scheme 1. The values are from Ref. [15].

Material	ρ (g/cm^3)	C_p (J/g °C)	λ (J/m s °C)
Glass	2.24	0.84	0.76
Rubber	0.95	2.1	0.15
Resin	1.15	1.88	0.29

Time condition: The system is initially ($t = 0$) at the uniform temperature, T_i, and is exposed to air at ambient temperature, $T_{amb} = T_i$

Boundary conditions ($t > 0$): In the centre of the mold $\partial T/\partial r = 0$ (this is a symmetry condition). The system is surrounded by air having a constant temperature, T_{amb}. The external surface of the mold is exposed to free convective air flow. Energy is carried or convected away by the air, and at the solid/air interface the energy transport is given by $hA(T_s - T_{amb})$, where h is the heat-transfer coefficient, A is the area normal to the direction of the heat flux, and $(T_s - T_{amb})$ is the difference between the temperature at the interface, T_s, and that in the ambient temperature. It was assumed that the temperature rise was not so large that the temperature dependence of the physical properties needed to be considered. The heat-transfer coefficient, evaluated under free convective air flow, was calculated to be 12.6×10^{-4} J/(s cm^2°C) [15]. The glass slide supporting the resin sample was in contact with the LED source. The thermal power produced by the LED was assessed as follows. A sample with an inserted thermocouple was "fully cured" under an extended photoirradiation and at an elevated temperature (the maximum was 100°C). After allowing the sample to cool to room temperature (20 ± 2°C), the sample was again irradiated and the temperature versus irradiation time was recorded. From the temperature evolution and the energy balance, the calculated thermal power of the LED was 18 mW/cm^2, assuming that heat production due to any additional polymerization was negligible.

The energy balance, coupled with the expression for the polymerization rate including attenuation of the light through the layer thickness and photobleaching of the photoinitiator, was solved by the forward Euler algorithm.

RESULTS AND DISCUSSION

Figure 1 shows the global (i.e., volume averaged) evolution of double bond conversion measured by NIR during photocuring of 1- and 2-mm thick samples containing 1 wt% CQ in combination with equimolar amount

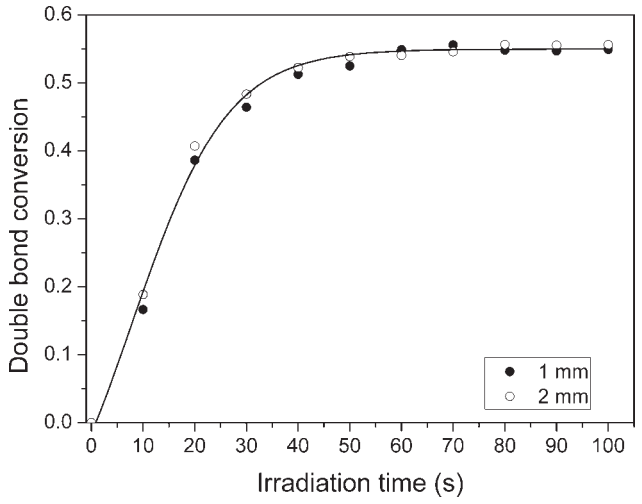

FIG. 1. Global (volume averaged) double bond conversion versus irradiation time measured in a sealed sample cell by NIR during nonisothermal polymerization of 1- and 2-mm thick samples of a 70:30 bis-GMA/TEGDMA blend containing 1 wt% CQ in combination with equimolar amount of DMAEMA.

of DMAEMA using a 5 mW/cm^2 radiation source and exposure periods of 10–100 s.

Surprisingly, despite the differing extent of radiation attenuation by the CQ as a function of depth, no significant differences were observed between layers of different thickness. Previously reported measurements of double bond conversion obtained from volume shrinkage measurements of 1- and 2-mm thick samples performed under continuous irradiation with an intensity of 5 mW/cm^2 are presented in Fig. 2 [12]. The advantage of the volume shrinkage technique is that it permits the continuous monitoring of the evolution of double bonds conversion during irradiation. In addition, temperature rise and radiation attenuation through the sample during polymerization can be assessed in similar test specimens to those used in the volume shrinkage measurements.

The conversion and rate rata under continuous irradiation (Fig. 2) are lower than that measured by the NIR technique (Fig. 1). This is attributed to the exposure of the surface of the specimens in the setup shown in Scheme 1 to an air atmosphere, which retards the polymerization of the samples when compared with the NIR experiments in which the resin was enclosed. In addition, the different molds used in the NIR and the setup shown in Scheme 1 resulted in different cure temperature and consequently slightly different final monomer conversion between both techniques. In agreement with NIR measurements (Fig. 1), no difference in the conversion of samples of different thickness was observed under continuous irradiation (Fig. 2) despite the different extent of radiation attenuation by the CQ as a function of depth. The observed anomaly suggests that competing factors are producing this overall independence of cure rate and final conversion on sample thickness.

A common characteristic of photopolymerization reactions is a nonuniformity of the reaction rate, due to the dependence of rate on local light intensity and photoinitiator concentration [5–7]. As light is absorbed along the optical path, at any time, the light intensity will be a function of position in the specimen. In addition, the photoinitiator CQ is photobleached during irradiation so that the light penetrates more deeply into the sample as the irradiation time is extended. In this study, the local initiation rates were computed from the general relationships for spatiotemporal variation of the concentration of the photobleaching initiator in systems where light attenuation and initiator consumption are considered. The light intensity decreases along the beam direction according to the integrated form of the Beer–Lambert law:

$$I(z,t) = I_0 \exp\left[-\int_0^z \varepsilon\, \mathrm{CQ}(z,t)dz\right] \tag{2}$$

where $I(z,t)$ is the local light irradiance (in units of moles of photons per unit time per area), I_0 is the incident light irradiance, CQ is the molar concentration of CQ, ε is the wavelength dependent Neperian absorption coefficient of CQ (97 l mol^1 cm^1 at 470 nm) equal to 2.302 times its decadic extinction coefficient and z is the position into the depth of the material. The symbols used in computations are presented in Table 2. It should be noted that for a polychromatic radiation source, *Eq. 2* should be replaced by an integral of the intensity over the wavelength range [16]. The local decomposition rate of CQ is proportional to the volumetric rate of absorption of photons:

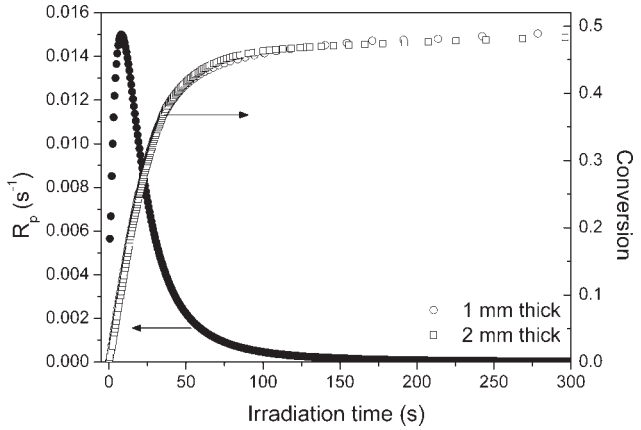

FIG. 2. Global (volume averaged) double bond conversion and polymerization rate versus irradiation time reported in Ref. [12]. The measurement was carried out during continuous nonisothermal polymerization in an open sample cell with 1- or 2-mm thick samples of a 70:30 bis-GMA/TEGDMA blend containing 1 wt% CQ in combination with equimolar amount of DMAEMA. No differences between the conversion plots for the 1- and 2-mm thick samples are observed. The polymerization rate data is plotted only for the 1-mm thick sample to make the plot clearer.

DOI 10.1002/pen

TABLE 2. Symbols used in computations.

Symbol	Quantity	Units
z	Layer depth or position in layer	M
Φ	Quantum yield of CQ consumption	
ε	Neperian absorption coefficient of CQ	M^{-1} m^{-1}
I_0	Incident light irradiance	mW cm^{-2}
$I(z)$	Local light irradiance	mW cm^{-2}
$\Phi\varepsilon I_0$	Rate constant for the photobleaching of CQ	s^{-1}
$M(z)$	Local double bonds concentration	M
M_g	Layer-averaged double bonds concentration	M
$x(z)$	Local double bond conversion	
X_g	Layer-averaged double bond conversion	
R_p	Local polymerization rate	M s^{-1}
R_{pg}	Layer-averaged polymerization rate	M s^{-1}
k_p	Propagation kinetic coefficient	M^{-1} s^{-1}
k_t	Termination kinetic coefficient	M^{-1} s^{-1}

$$\frac{\partial CQ}{\partial t} = \Phi\ \varepsilon\ I(z,t)CQ(z,t) \tag{3}$$

where Φ is the quantum yield of the photoinitiator consumption. From the system of *Eqs. 2* and *3*, it is clear that optical attenuation and photoinitiator consumption result in a spatiotemporal variation of photoinitiation rates and, consequently, a distribution of polymerization rate through the specimen thickness. Computations of local concentration of CQ require the knowledge of its photobleaching rate constant. Assuming a first-order rate of CQ loss, for a thick sample, the global rate of decomposition of CQ is related to the quantum yield and the radiation absorbed [5, 17]:

$$-\frac{dCQ}{dt} = \frac{\Phi I_{abs}}{L} = \frac{\Phi I_0(I - e^{-\varepsilon L\, CQ})}{L} \tag{4}$$

where L is the sample thickness. By integrating *Eq. 4* yields:

$$\ln\left[\frac{(10^{\varepsilon LCQ} - I)}{(10^{\varepsilon LCQ_0} - I)}\right] = \Phi\ \varepsilon\ I_0\ \ t \tag{5}$$

where $\Phi\varepsilon I_0$, is the rate constant for the photobleaching of CQ. The values of the ordinate were calculated assuming a decrease in the transmitted light intensity according to the Beer–Lambert law. Figure 3 shows the plot of *Eq. 5* from transmitted light measurements at 5 mW/cm^2. The rate constant for the photobleaching of CQ, calculated from the slope of the resulting line, was 0.0014 s^1. The influence of irradiance and sample thickness on the photobleaching rate of CQ was reported elsewhere [18].

The rate of free-radical polymerization is given by the product of the propagation rate constant, the radical concentration and monomer concentration [17]. Under the steady state hypothesis for the radical concentration, the local polymerization rate, R_p, is given by [3, 17]:

$$R_p(z,t) = -\frac{\partial M(z,t)}{\partial t} = \frac{k_p}{k_t^{1/2}}[f\ \Phi\ \varepsilon\ I(z,t)CQ(z,t)]^{1/2}\ \ M(z,t) \tag{6}$$

where the initiation efficiency, f, is the number of primary radicals produced from the CQ decomposition, M is the molar double bond concentration, and k_p and k_t are the propagation and termination kinetic coefficients. Thus, from the solution of *Eqs. 2–4*, the photoinitiator concentration, light intensity, and monomer concentration can be calculated as a function of time and position. In what follows, the local monomer conversion profiles along the irradiation path are calculated from the global conversion measurements (see Fig. 2) carried out under nonisothermal conditions. The global (volume averaged) reaction rate during a time increment dt can be expressed in terms of the local reaction rate at each depth z as follows:

$$R_{pg} = \frac{1}{L}\int_0^L R_p(z) = \frac{1}{L}\int_0^L \frac{k_p(z)}{k_t(z)^{1/2}}[f(z)\Phi\,\varepsilon I(z)CQ(z)]^{1/2}\,M(z)dz \tag{7}$$

As the change in conversion in a small time interval is proportional to the rate of polymerization, the change in the concentration of double bonds in a layer of thickness dz at a depth z during a time increment dt is related with the change in the global (or volume averaged) concentration of double bonds by the following relationship:

$$\frac{dM(z)}{dM_g} = \frac{\dfrac{k_p(z)}{k_t^{1/2}(z)}[f(z)\Phi\,\varepsilon I(z)CQ(z)]^{1/2}\,M(z)}{\dfrac{1}{L}\displaystyle\int_0^L \frac{k_p(z)}{k_t^{1/2}(z)}[f(z)\Phi\,\varepsilon I(z)CQ(z)]^{1/2}\,M(z)dz} \tag{8}$$

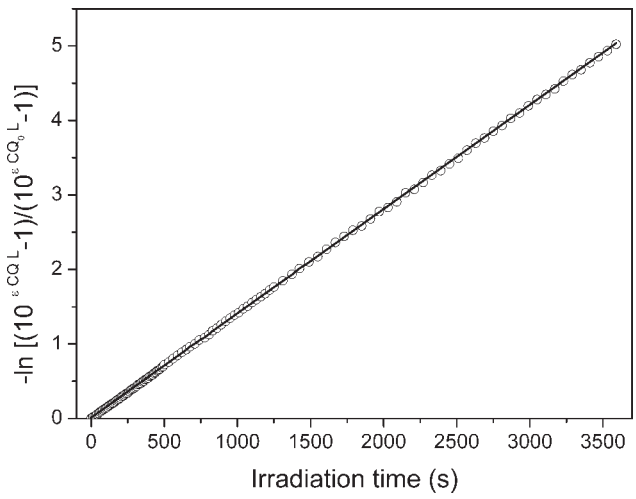

FIG. 3. Plot of *Eq. 5* from transmitted light measurements in about 1-mm specimen of a 70:30 bis-GMA/TEGDMA blend containing 1 wt% CQ in combination with equimolar amount of DMAEMA. The irradiance was 5 mW/cm^2.

where $dM(z)$ is the change in double bond concentration at a depth z, dM_g is the total change in double bond concentration averaged over the sample thickness, and L is the sample thickness. The direct relation between conversion and monomer concentration gives the change in conversion, $dx(z)$, in a layer of thickness dz at a depth z during a time increment dt, relative to the change in global conversion, dX_g:

$$\frac{dx(z)}{dX_g} = \frac{dM(z)}{dM_g} \tag{9}$$

Computation of double bond conversion profiles along the layer thickness from *Eqs. 8* to *9* requires a knowledge of the kinetics of decomposition of the photoinitiator, the photoinitiator efficiency and the values of k_p and k_t. Polymerization of multifunctional dimethacrylates exhibit complex behavior due to the fact that the kinetics depends on the mobility of the medium which changes during the process [19–21]. Figure 2 shows the characteristic curing behavior of a 70:30 bis-GMA/TEGDMA blend photopolymerization. The data illustrates autoacceleration immediately after irradiation commences so that the reaction rate reaches a maximum value at a double bond conversion of about 10%. A similar increase in the reaction rate at the beginning of the reaction has also been observed under isothermal measurements and has been attributed to diffusion limitations of the termination process [9]. As the polymerization progresses, the polymer molecular weight increases and gelation occurs so that the mobility of the environment decreases resulting in a reduction in the termination rate constant and the initiation efficiency and an increase in reaction rate as shown in Fig. 2. The photoinitiator in the present system is not totally consumed even at the end of the reaction. Thus the observed rapid drop in the cure rate and the failure of the system to attain full conversion (Fig. 2) is due to a vitrification effect where the propagation reaction also becomes diffusion controlled because the temperature of the system approaches the conversion dependent glass transition temperature (T_g). At this stage, the reaction rate approaches zero within the time scale of the experiment. These diffusion controlled kinetics of the system lead to, k_p, k_t, and f values that are function of the medium mobility. Thus, correct computation of the monomer concentration as a function of depth into the sample requires the knowledge of the relationship of k_p, k_t, and f with monomer conversion and temperature. If it is assumed that differences in conversion as a function of depth are not large so that all of the sample is under the same diffusion control regime, then the change in local monomer conversion in a time interval dt can be calculated from the global (volume averaged) conversion measured, dX_g, by the following relationship:

$$dx(z) = \frac{\frac{k_p(z)}{k_t^{1/2}(z)}[f(z)\Phi\varepsilon I(z)\mathrm{CQ}(z)]^{1/2} M(z)}{\frac{1}{L}\int_0^L \frac{k_p(z)}{k_t^{1/2}(z)}[f(z)\Phi\varepsilon I(z)\mathrm{CQ}(z)]^{1/2} M(z)dz} dX_g \tag{10}$$

which can be simplified by cancellation of Φ and ε and re-expressed in terms of discrete variables as follows

$$\Delta x(z) = \frac{L}{\Delta z}\frac{[I(z)\mathrm{CQ}(z)]^{1/2} M(z)}{\sum_{z=0}^{z=L}[I(z)\mathrm{CQ}(z)]^{1/2} M(z)}\Delta X_g \tag{11}$$

Here, the conversion profiles are only dependent on the local photoinitiation rates, that is, light intensity and local concentration of CQ. *Equation 11* was incorporated into the coupled system of energy balance *Eqs. 1–3* and these were solved to compute local temperature and local double bond conversion as a function of irradiation time from the previously determined rate constant for the photobleaching of CQ, that is, $\Phi\varepsilon I_0 = 0.0014\ s^1$ and the experimentally determined global monomer conversion shown in Fig. 2. Figure 4 illustrates the local monomer conversion for 1- and 2-mm layers of a 70:30 bis-GMA/TEGDMA blend containing 1 wt% CQ in combination with DMAEMA. As expected,

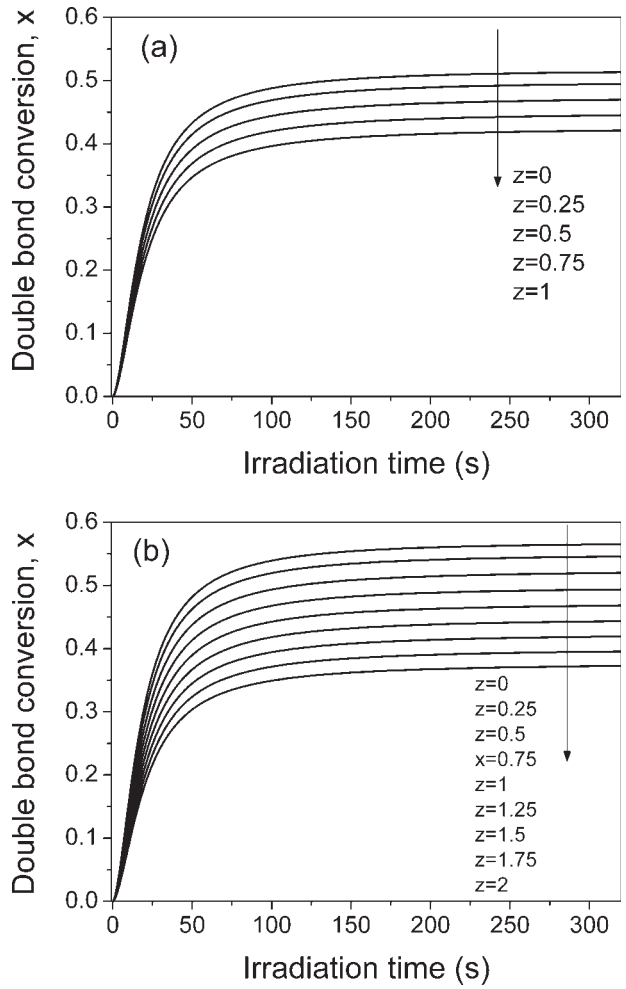

FIG. 4. (a) Local conversion profiles in a 1-mm thick sample of a 70:30 bis-GMA/TEGDMA blend containing 1 wt% CQ in combination with DMAEMA. Computations were carried out using *Eq. 11* and the global experimental measurements presented in Fig. 2. (b) Local conversion profiles in a 2-mm thick sample. *Ibid* Fig. 4a.

 DOI 10.1002/pen

these plots show that the conversion decreases at greater depths into the sample due to the attenuation of the radiation by overlying layers of resin. However, Fig. 4 also reveals that the conversion at a certain depth into the material also depends on the thickness of the specimen as indicated by the difference in the conversion profiles at the irradiation surface of the two specimens. This indicates that another factor—that of temperature exotherm—is responsible of the spatiotemporal monomer conversion distribution, in addition to light attenuation and CQ photobleaching.

Figure 5 show the temperature profiles calculated with the energy balance (*Eq. 1*) and the data presented in Fig. 4 during polymerization in a 1- and 2-mm thick specimens of a 70:30 bis-GMA/TEGDMA blend containing 1 wt% CQ in combination with DMAEMA. In the early stages of the photopolymerization, a sharp temperature rise is observed caused by the exothermic reaction during the initially fast polymerization. At this stage, the rate of heat transfer by conduction and convection is much lower than the rate of heat production; therefore, a considerable part of the energy liberated is accumulated into the system as temperature rises. When the reaction rate passes through a maximum due to monomer consumption and diffusional effects on the initiation efficiency and the propagation and termination rates, the rate of heat transfer competes with the rate of heat production and the increase in temperature is less rapid. Finally, as the double bond conversion approaches a plateau due to vitrification of the resin, the rate of heat production becomes negligible compared with the rate of heat transfer, and so the temperature decreases rapidly. For the resin in contact with the glass slide, the temperature changes are moderated by heat exchange at the resin/glass interface; therefore, the peak temperature at this point is lower than that in the resin/air interface. Because of the different thermal properties of glass and air, the temperature gradient in the resin close to the glass substrate is relatively pronounced whereas the peak temperature of the resin closer to the air-resin interface changes by $<1^{\circ}$C. It is worth noting that in the resin at the air-resin interface, that is, where the photoinitiation rate is reduced due to attenuation of the overlying resin layers, the cure temperature is substantially higher than that at the irradiation surface and the difference is more marked when the layer thickness increases.

The temperature evolution of the theoretical computations of temperature (calculated with the monomer consumption profiles presented in Fig. 4) during photopolymerization is compared with experimental results in Fig. 6 for 1.1- and 2.03-mm thick layers. In the final region in Fig. 6, the LED was turned off and the removal of this heat source resulted in a faster cooling of the sample. The good agreement between the theoretically computed and experimental exotherm measurements confirms the validity of the approach used to predict the local polymerization rates in samples of different thickness.

In contrast with thermally activated polymerizations, in which the higher the cure temperatures the higher

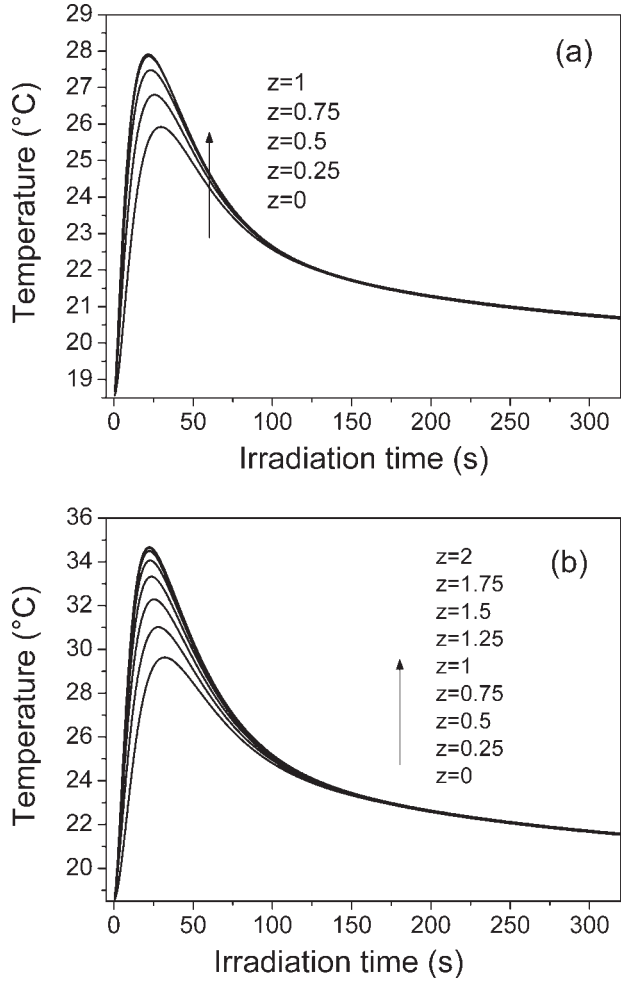

FIG. 5. (a) Local temperature evolution calculated with the energy balance (*Eq. 1*) during polymerization in a 1-mm thick sample of a 70:30 bis-GMA/TEGDMA blend containing 1 wt% CQ in combination with DMAEMA. Local changes in conversion with time were computed from *Eq. 11*. (b) *Ibid* Fig. 5a for a 2-mm thick sample.

the monomer consumption [22], in photopolymerized systems a same overall monomer conversion may be accompanied by different thermal histories. From these results, it may be concluded that for the experimental conditions used in this study, cure temperature and light attenuation have counteracting effects resulting in the same overall conversion averaged over the thickness although the monomer profiles along the thickness is markedly different.

As described earlier, k_p, k_t and the initiator efficiency depend on the molecular mobility and so are dependent on temperature and double bond conversion. On the other hand, the rate of decomposition of a photoinitiator is not dependent on temperature. After a certain irradiation time and at a given depth z into the 1- and 2-mm thick layers, the radiation intensity, $I(z)$, and photoinitiator concentration, CQ(z), are constant. In addition, for the same local conversion in the 1- and 2-mm samples, the composite rate constant, fk_p/k_t [1/2], is only dependent on the local

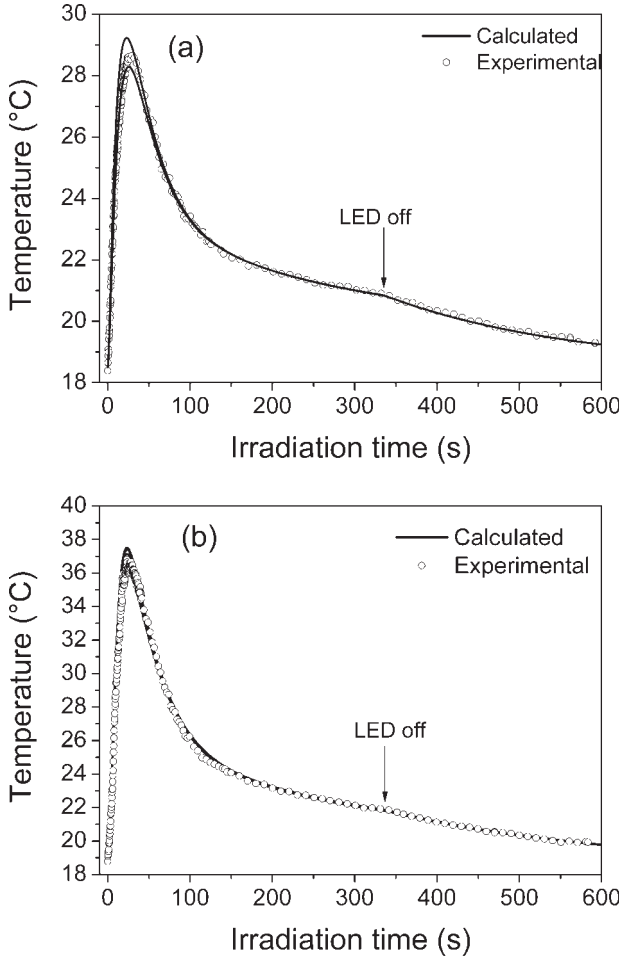

FIG. 6. (a) Measured and calculated temperature progress at a position of about $z = 0.75$ mm during polymerization in a 1.1-mm thick sample. (b) Measured and calculated temperature progress at a position of about $z = 1.5$ mm during polymerization in a 2.03-mm thick sample.

temperature. Therefore, *Eq. 6* shows that the ratio of the local polymerization rate for the 1- and 2-mm thick samples calculated at a same depth and at a same monomer conversion will be only function of the local temperature. Under this condition, the dependence of the kinetic coefficients with the cure temperature can be assessed. Assuming that the reaction rate follows the Arrhenius behavior, the overall activation energy of the reaction can be calculated from the local polymerization rates calculated at a same depth and for a same double bond conversion as follows:

$$\frac{R_{\mathrm{p1mm}}}{R_{\mathrm{p2mm}}} = \frac{\left(f^{1/2}k_{\mathrm{p}}/k_{\mathrm{t}}^{1/2}\right)_{1\mathrm{mm}}}{\left(f^{1/2}k_{\mathrm{p}}/k_{\mathrm{t}}^{1/2}\right)_{2\mathrm{mm}}} = \frac{\exp(-E_{\mathrm{A}}/R\,T_{1\mathrm{mm}})}{\exp(-E_{\mathrm{A}}/R\,T_{2\mathrm{mm}})} \qquad (12)$$

and

$$\ln\left(\frac{R_{\mathrm{p1mm}}}{R_{\mathrm{p2mm}}}\right) = -\frac{E_{\mathrm{A}}}{R}\left(\frac{1}{T_{1\mathrm{mm}}} - \frac{1}{T_{2\mathrm{mm}}}\right) \qquad (13)$$

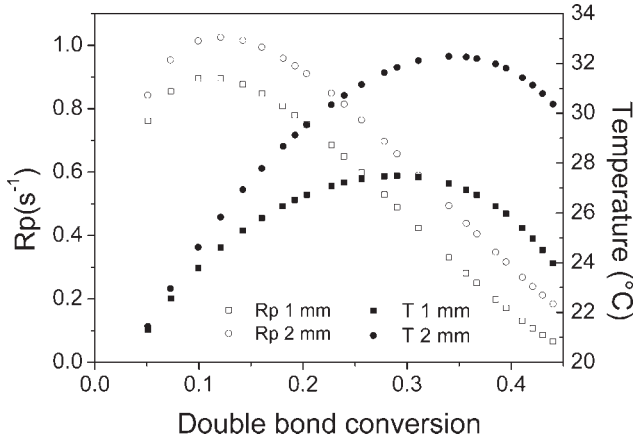

FIG. 7. Polymerization rate and temperature at a depth z equal to 0.5 mm in 1- and 2-mm thick samples as a function of conversion.

where R_{p1mm} and R_{p2mm} are the local polymerization rates at the same depth z in the 1- and 2-mm thick layers, respectively. The values of R_{p} and temperature were calculated from *Eqs. 11* and *1*, respectively, at a depth of 0.5 mm for a same conversion in the 1- and 2-mm thick layers and the results are depicted in Fig. 7. From the rate versus temperature data in Fig. 7, the Arrhenius activation energy of the polymerization can be computed. As shown in Fig. 8, a linear plot is observed during the initial part of the reaction with an overall activation energy of 25 kJ/mol. This value is in agreement with that reported by Lovell et al. [10] for isothermal photopolymerization of a 50:50 wt% bis-GMA/TEGDMA blend. The plot is linear up to a conversion of about 20%, after which the traces become curved. This behavior may be attributed to a nonchemical dependence of the rate coefficients when they become diffusion controlled.

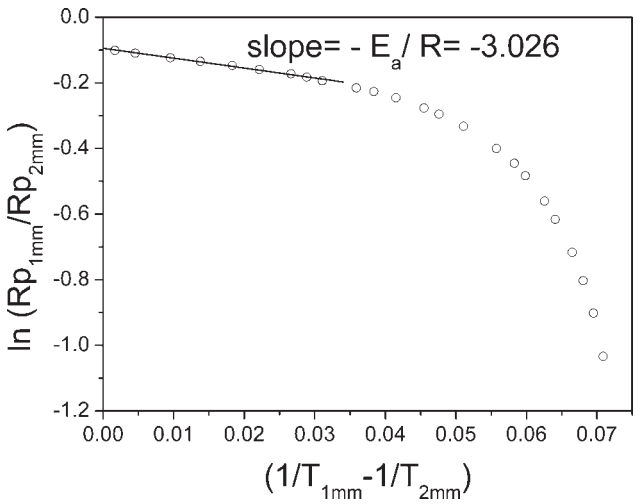

FIG. 8. Arrhenius plot calculated from data presented in Fig. 7. The activation energy calculated from the slope of the initial line was 25 kJ/mol. The plot is linear up to a conversion of about 20%.

DOI 10.1002/pen

CONCLUSIONS

In this work, the influence of sample thickness and thermal boundary conditions on the progress of local monomer conversion and local temperature exotherms during light-initiated polymerization of a bis-GMA/TEGDMA resin was studied. Local photoinitiation rates were calculated from the spatiotemporal variation of the photoinitiator concentration and light intensity. Gradients of monomer conversion profiles were assessed from measured conversion profiles averaged over the sample thickness by taking into account the spatiotemporal variation of the photoinitiator rate.

Theoretical computations of the evolution of the temperature in samples of different thickness were in satisfactory agreement with experimental measurements and from this data, the Arrhenius activation energy in the early stages of the reaction was determined to be 25 kJ/mol. From the results presented, it emerges that the sample thickness and thermal boundary conditions control the relative rates of heat generation and heat transfer, and consequently the cure temperature. The higher peak temperature was attained in the thickest sample, bringing about increased polymerization rate and, in turn, increased double bond conversion. However, the increased cure temperature was accompanied by more light attenuation, which creates regions of lower polymerization degree. This means that light attenuation and local temperature counteract with one another, and under the conditions used for this study, no differences in the global monomer conversion were observed for samples with different thicknesses. Thus, this research highlights the inherent interlinking of thermal and radiation attenuation effects in bulk photopolymerizing systems.

ACKNOWLEDGMENTS

The financial support provided by the CONICET, ANPCyT through Grant PICT 00550 is gratefully acknowledged. The authors are grateful to Esstech for the donation of the Bis-GMA monomer used in this study.

REFERENCES

1. W.D. Cook, *Polymer*, **33**, 600 (1992).
2. W.F. Shroeder and C.I. Vallo, *Dent. Mater.*, **23**, 1313 (2007).
3. P. Xiao, Y. Wang, M. Dai, S. Shi, G. Wu, and J. Nie, *Polym. Eng. Sci.*, **48**, 884 (2008).
4. J.P. Fouassier, *Polym. Eng. Sci.*, **35**, 1061 (1995).
5. G. Terrones and A.J. Pearlstein, *Macromolecules*, **34**, 3195 (2001).
6. A.K. O'Brien and C.N. Bowman, *Macromolecules*, **36**, 7777 (2003).
7. A.K. Cabral and J.F. Douglas, *Polymer*, **46**, 4230 (2005).
8. L. Xu and L.J. Lee, *Polym. Eng. Sci.*, **45**, 496 (2005).
9. T.F. Scott, W.D. Cook, and J.S. Forsythe, *Polymer*, **43**, 5839 (2002).
10. L.G. Lovell, K.A. Berchtold, J.E. Elliott, H. Lu, and C.N. Bowman, *Polym. Adv. Technol.*, **12**, 335 (2001).
11. C.E. Corcione, A. Greco, and A. Maffezzoli, *Polym. Eng. Sci.*, **46**, 493 (2006).
12. V. Mucci, G. Arenas, R. Duchowicz, W.D. Cook, and C.I. Vallo, *Dent. Mater.*, **25**, 103 (2009).
13. M. Trujillo, S.M. Newman, and J.W. Stansbury, *Dent. Mater.*, **20**, 766 (2004).
14. R.B. Bird, W.E. Stewart, and E.N. Lightfoot, *Transport Phenomena*, 2nd ed., John Wiley, New York (2002).
15. M.N. Özisic, *Basic Heat Transfer*, McGraw-Hill, New York (1975).
16. W.F Schroeder, W.D Cook, and C.I. Vallo, *Dent. Mater.*, **24**, 686 (2008).
17. G. Odian, *Principles of Polymerization*, 2nd ed., John Wiley, New York (1981).
18. S. Asmussen, G. Arenas, W.D. Cook, and C.I. Vallo, *Eur. Polym. J.*, **45**, 515 (2009).
19. S.H. Dickens, J.W. Stansbury, K.M. Choi, and J.E. Floyd, *Macromolecules*, **36**, 6043 (2003).
20. K.A. Berchtold, T.W. Randolph, and C.N. Bowman, *Macromolecules*, **38**, 6954 (2005).
21. E.R. Soulé, J. Borrajo, and R.J.J. Williams, *Polym. Eng. Sci.*, **46**, 1641 (2006).
22. C.I. Vallo, *J. Biomed. Mater. Res. Appl. Biomater.*, **63**, 627 (2002).